Water-Filling Characteristics and Water Source of Weakly Rich Water and Weakly Conducting Water Aquifers in the Changxing Formation after Mining Damage

Xianzhi Shi , Guosheng XU * , Shuyun ZHu

Posted Date: 13 May 2024

doi: 10.20944/preprints202402.0266.v2

Keywords: Changxing Formation limestone; mining-induced fractures; mine water-inrush source; atmospheric precipitation

Article

Water-Filling Characteristics and Water Source of Weakly Rich Water and Weakly Conducting Water Aquifers in the Changxing Formation after Mining Damage

Xianzhi Shi [1,2], Guosheng Xu [3,*] and Shuyun Zhu [1]

[1] School of Resources and Earth Science, China University of Mining and Technology, Xuzhou 221116, China; zslsxz@aliyun.com (X.S.); shyzhuqiao@163.com (S.Z.)
[2] Guizhou Yuxiang Mining Group Investment Co. Ltd., Bijie 551800, China
[3] College of Mining Engineering, Guizhou University of Engineering Science, Bijie 551700, China
* Correspondence: jzxgsheng@126.com

Abstract: The escalation of mining activities in the karst regions of Guizhou Province has heightened the occurrence of water-inrush incidents in deep coal mines. This study focused on water-inrush phenomena within the Xinhua mining area of Jinsha County, Guizhou Province, aiming to investigate the sources of these incidents. The findings indicated that the overlying limestone of the Changxing Formation in the coal seam served as a vulnerable aquifer under certain conditions, leading to water inrushes. The analysis of the spatiotemporal distribution patterns of water-inrush incidents at the working face indicated that previous mining operations damaged the shallow Changxing Formation limestone, resulting in the accumulation of goaf water and the formation of numerous mining-induced fractures. These fractures served as rapid conduits for water inrushes from both atmospheric precipitation and underground sources at the deep working face. The examination of surface water and mine water quality demonstrated that both exhibited similar characteristics, predominantly featuring bicarbonate, sulfate, and sodium compositions. Investigation into the relationship between mine water inflow and atmospheric precipitation established that atmospheric precipitation influenced the mine water supply cycle, with a replenishment period of ~10 months during the operational phase of the Jinyuan Coal Mine and about one month post-closure. The fractures induced by mining activities within the Changxing Formation limestone facilitated water flow, with atmospheric precipitation serving as the primary water source for the mine. This study offered a valuable scientific foundation for addressing water-related damage resulting from atmospheric precipitation in mines susceptible to water inrushes under analogous hydrogeological conditions.

Keywords: Changxing Formation limestone; mining-induced fractures; mine water-inrush source; atmospheric precipitation

1. Introduction

Guizhou Province serves as the main coal production hub in the karst areas of southwestern China, where atmospheric precipitation stands out as a crucial water supply source during coal mining [1–4]. A clear correlation exists between mine water inflow and atmospheric precipitation, particularly evident in coal seams proximate to shallow outcrops. However, as mining operations extend into deeper coal seams, the intensity of atmospheric precipitation recharge diminishes significantly, resulting in a less pronounced correlation [5]. Notably, the Xinhua mining area features extensive surface outcrops of the Changxing Formation limestone, facilitating direct replenishment from atmospheric precipitation and indirect water-filling within the mining area. The Changxing Formation limestone area, characterized by a weakly rich (permeable) water-bearing layer, enhances high water content in local structures as well as the proliferation of karst gaps and caves. Thus, it serves as a conduit for channeling atmospheric precipitation to supply deep mining areas. Notably,

mines near coal seam outcrops have not experienced water-inrush incidents during the mining process. However, with the expansion of goaf areas and mining intensity, certain mines operating in deep coal seams have encountered roofwater-inrush incidents, resulting in the flooding of working faces and casualties.

Several studies have analyzed the correlation between mine water inflow and atmospheric precipitation, indicating that atmospheric precipitation is the source of mine water inflow in shallow coal seams in southwestern karst mining areas [3,6]. However, there seems to be a lack of research concerning water inflow due to deep coal seams during mining operations. Researchers such as Mo Lianhong, Fan Juan, and others [7] conducted inorganic and organic hydrochemical analysis in the Xiaotun mining area, focusing on utilizing atmospheric precipitation as a mine recharge water source. Furthermore, this method accurately analyzes the water source for mine recharge, but its complex application impedes broader application by on-site engineering and technical personnel. Different scholars have explored drilling [8,9], researched supply channels [5,10], and employed various methodologies to study the water source for mine roofs, offering guidelines for mitigating atmospheric precipitation recharge in mines. However, the engineering complexity or high technical difficulty associated with these methods inhibits the mastery of on-site engineering and technical personnel, thus limiting practical applications. Certain scholars have proposed water separation methods to supply mines by studying the separation space between Changxing Formation limestone and Longtan formation strata [11,12]. Despite clear reasons for mine water inrush, no research has delved into the continuous water inflow source from the working faces.

This study investigated the spatiotemporal relationship between different water-inrush mines, water-inrush working faces, and goaf within the Xinhua mining area. Furthermore, employing comprehensive methodologies such as hydrochemical analysis coupled with the assessment of atmospheric precipitation recharge timing and intensity, existing hydrogeological data from mines were collected and analyzed to design recharge channels and water storage spaces originating from atmospheric precipitation. The results were instrumental in determining the hydrochemical relationship between atmospheric precipitation and mine water, as well as the correlation between mine water inflow and atmospheric precipitation. Interestingly, this study analyzed atmospheric precipitation as the water source for inrush incidents in the deep mining face of the area. For the first time, the rapid replenishment mechanism of atmospheric precipitation in deep mines situated within weak aquifers and weakly conductive aquifers of the Changxing Formation limestone was studied. This study offered both theoretical and empirical bases for preventing and controlling atmospheric precipitation water damage in mines with similar hydrogeological conditions in karst development areas.

2. Overview of the Mining Area

2.1. Basic Information of the Mining Area

The Xinhua mining area (referred to as the mining area) is located in Jinsha County, Bijie City, Guizhou Province, southwest of Jinsha County, China. The mining area is ~220 km^2. All coal mines in the mining area are distributed in the northwest wing of the Jinsha Qianxi anticline and southeast of the exposed $15^{\#}$ coal seam (Figure 1). There are 39 pairs of production and construction mines in the mining area, with a designed production capacity of 0.3–1.5 million t/a per well and a single well area range of 1.81 km^2–90.02 km^2. Since 2010, employing comprehensive mechanized mining technology for raw coal production, the coal mines within the area have undergone resource integration and new mining rights establishment. These mines in the mining area have become dense, with a maximum of eight pairs of production mines oriented in the formation inclination direction.

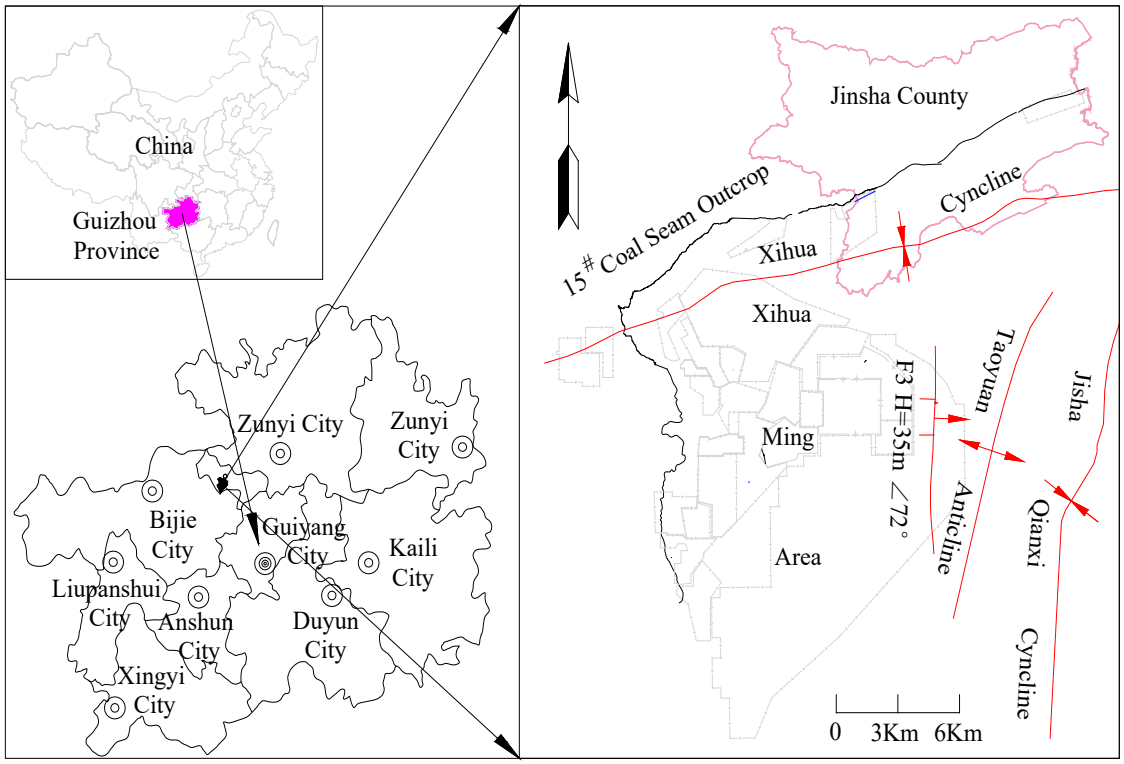

Figure 1. Map of the Xinhua mining area.

2.2. Introduction to Geology and Hydrogeology of the Mining Area

The main strata impacting coal-bearing strata mining in the Xinhua mining area, arranged from old to new, include the middle Permian Maokou Formation (P_2m), the upper Permian Longtan Formation (P_3l), the Changxing Formation (P_3c), the lower Triassic Yelang Formation (T_1y), and the Maocaopu Formation (T_1m), as well as the Quaternary (Q). The coal-bearing strata predominantly consist of the Permian Longtan Formation (P_3l).

The mining area is located on the west wing of the Jinsha Qianxi syncline, and the overall strata exhibit a monocline structure, with local undulations forming a secondary fold structure. Furthermore, during exploration and production activities, only one fault structure with a drop > 30 m was exposed near the southwest boundary of the mining area (within the Jinsha Longfeng Coal Mine scope). Subsequently, various coal mines have encountered small faults with varying drops. The strata within the mining area exhibited dip angles in the range of 65–155°, with dip angles in the range of 0–27°, with an average of 5–10°.

The Longtan Formation (P_3l) in the mining area constitutes a coal-bearing stratum primarily composed of gray and dark gray, thin to moderately thick layers of siltstone, sandy mudstone, and mudstone. It is interbedded with fine sandstone, calcareous mudstone, and 4–7 layers of limestone and mudstone. It contained 12–15 layers of coal and 2–6 layers of minable coal seams. Notably, the 4#, 9#, and 15# coal seams serves as the main mining coal seams in most mines, with the 5# coal seam being the most minable, exhibiting a thickness ranging from 0.45 m to 5.55 m and an average of 1.68 m. The thickness of the 9# coal seam varies from 0.59 m to 9.95 m, with an average of 2.77 m. The coal seam is positioned 39.70 m–76.22 m away from the Changxing Formation limestone, with an average of 53.31 m (Figure 2).

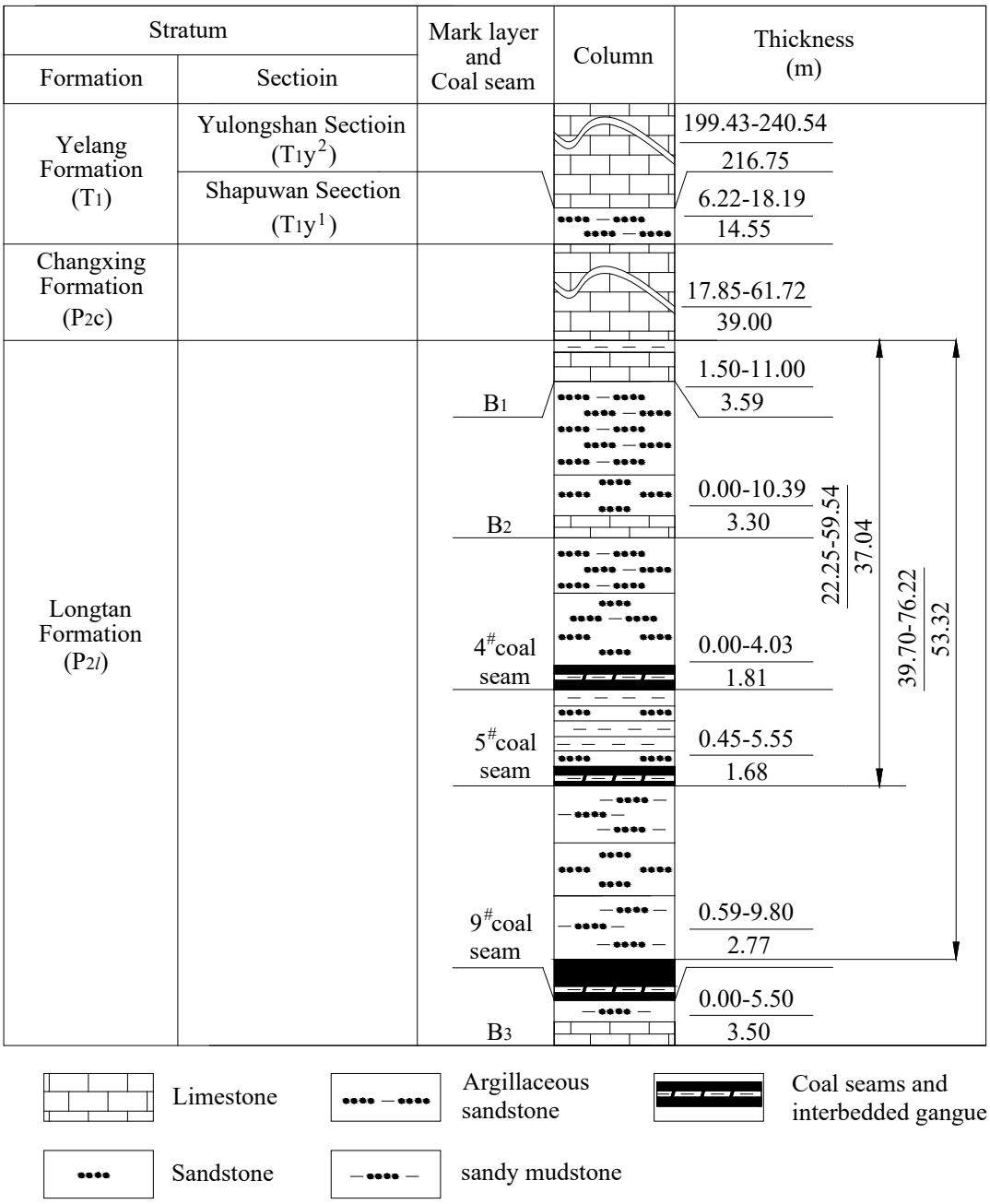

Figure 2. Comprehensive bar chart of coal-bearing strata in the Xinhua mining area.

The main aquifers within the mining area include the Triassic Yelang Formation Yulongshan section (T_1y^2) limestone, the Permian Changxing Formation (P_3c) limestone, and the Permian Maokou Formation (P_2m) limestone. The limestone within the Yulongshan section of the Triassic Yelang formation (T_1y^2) served as the main aquifer, exhibiting a thickness range of 176.62–248.3 m and an average of 211.92 m. The karst development of this aquifer varied significantly, making it a weak–strong aquifer with abundant water. The Shabaowan section (T_1y^1) served as a water barrier between the Yulongshan limestone and the coal-bearing strata below, with a thickness range of 7.45 m–211 m and an average of 14.91 m. The coal-bearing strata of the Longtan Formation (P_3l) served as weakly rich and impermeable layers. The aquifers directly filling water into the coal-bearing strata of the Longtan Formation were the overlying Changxing Formation limestone and the underlying Maokou Formation limestone. The limestone of the Changxing Formation (P_3c), in contact with the Longtan Formation strata, varied in thickness in the range of 17.85 m–61.72 m, with an average thickness of 39.00 m. The karst was underdeveloped, functioning as a weakly water-rich aquifer. Furthermore,

during mining activities targeting coal seams 9# and above, the Changxing Formation limestone aquifer emerged as the primary aquifer influencing mine safety. The analysis of exploration data from various coal mines within the area indicated a third type of mineral deposit exploration, with the first type being karst water-filled deposits with simple hydrogeological conditions.

2.3. Hydrogeological Characteristics of Limestone in the Changxing Formation

The Changxing Formation limestone is extensively developed in the entire area, exhibiting a thickness range of 17.85–61.72 m with an average of 39.00 m. Lithologically, the strata are mainly composed of gray to dark gray, medium to thickly layered chert limestone, and thickly layered limestone. The Changxing Formation limestone is prominently exposed across the surface of most mines within the mining area (Figure 3), characterized by generally low-lying terrain and locally developed small karst depressions, sinkholes, and cliffs. Boreholes constructed by various coal mines during exploration activities in the mining area have exposed this limestone layer, indicating an effective karst rate ranging from 1.2% to 1.6%. Locally, the limestone contained karst caves, with recorded cave heights ranging from 0.18 m to 8.74 m. Notably, some caves were filled with yellow mud. The partial leakage of the limestone was exposed during drilling operations, exhibiting a leakage rate of 17.5%. The depths of the leakage points were <367.4 m, with the lowest elevation at 922.16 m.

Research results by Li Bo et al. [13] and Shi Xianzhi et al. [14] indicated that the water level of the limestone aquifer in the mining area was significantly affected by terrain, surface weathering, and erosion. Consequently, the highest water level of the Changxing Formation limestone reached 1436.62 m, and the lowest was 1063.59 m. The pumping test data of various coal mines within the Xinhua mining area indicated that only one borehole (Linhua Coal Mine) in the Changxing Formation limestone measured a unit water inflow q of 0.1418 L/m·s, while the rest of the boreholes were between 0.0000041 L/m·s and 0.0127 L/m·s. The hydraulic conductivity K measured by the pumping test of only one borehole in the mining area was 0.1079 m/d, while the other boreholes were between 0.0000026 m/d and 0.004 m/d.

Furthermore, based on comprehensive analysis, the limestone of the Changxing Formation was identified as generally exhibiting weak water richness and weak water conductivity, with poorly connected dissolution gaps. In areas with well-developed structures, karst development and water abundance led to water inrush during mining operations. The limestone of the Changxing Formation is commonly exposed within the mining area and is replenished by atmospheric precipitation. Studies by Shi Xianzhi et al. [5], Yao Guanghua et al. [15], Wang Zaiyong et al. [16], Long Tianwen et al. [17], and Xiao Lele et al. [18] have shown that under conditions of fracture development due to mining activities, the limestone of the Changxing Formation supplied the mining site through channels such as karst and fractures.

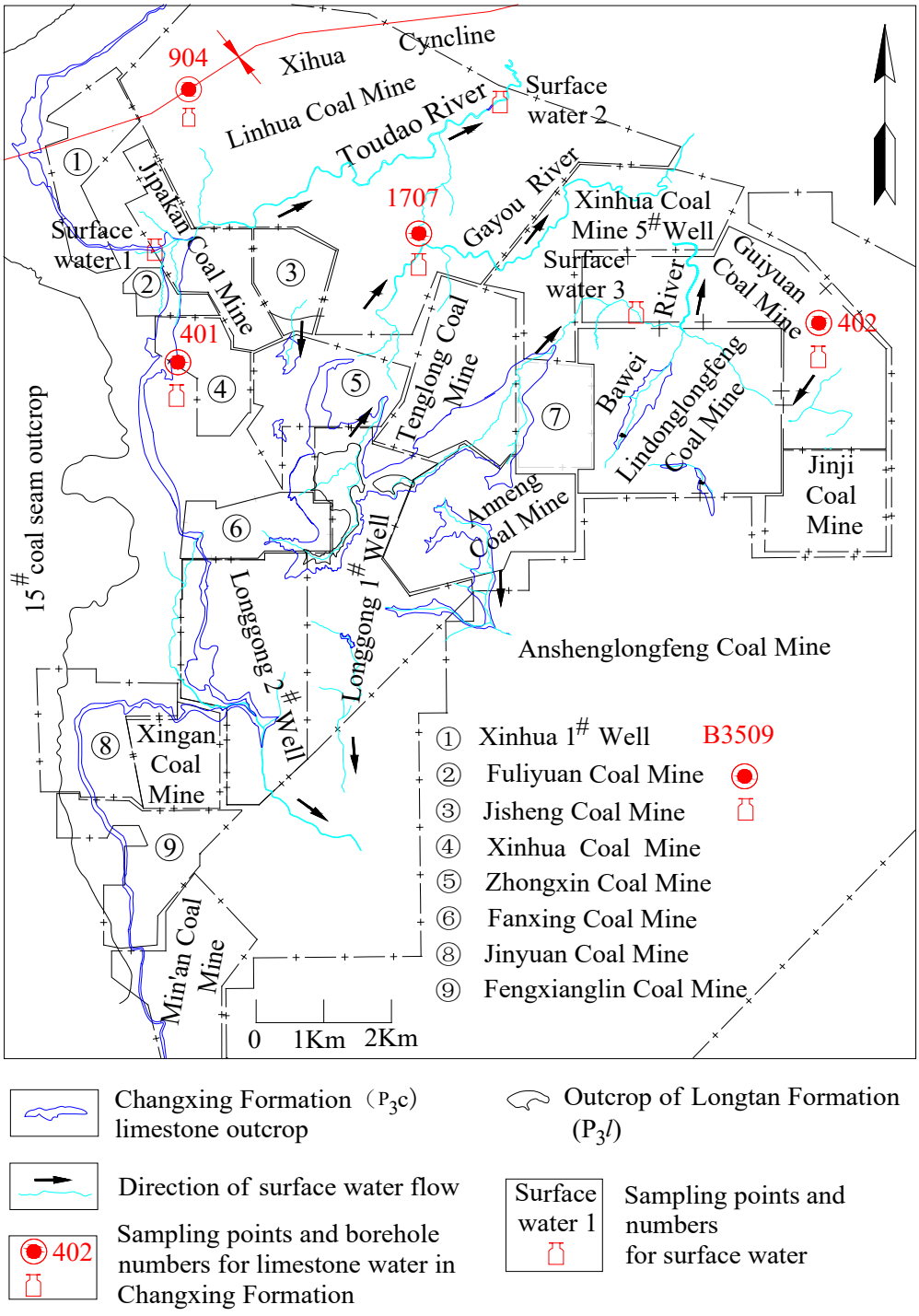

Figure 3. Layout plan of Changxing Formation outcrop distribution and groundwater sample locations.

2.4. Water-Inrush Situation in Coal Mines in the Mining Area

Since April 2016, comprehensive mechanized coal mining technology has been widely applied in various mines within the mining area, leading to significant improvements in the mining height and scale of coal seams. As the mining scope of each mine expanded and the number of closed pit mines increased, it was observed that the occurrence of water-inrush incidents in the mining area gradually increased. In the mining area, Linhua Coal Mine, Jinji Coal Mine, Guiyuan Coal Mine, Longfeng Coal Mine of Lindong Company, Tenglong Coal Mine, and others exhibited water inrush from the roof of the 9# coal seam working face. This has seriously affected the safety production of

the mine. According to the mining data from the 9# coal seam working face in each mine, the mining height of the 9# coal seam was in the range of 2.2 m–3.5 m. Additionally, during the production period of the working face, normal water inflow rates ranged from 20 m^3/h to 470 m^3/h, while instances of water inrush generally ranged from 80 m^3/h to 800 m^3/h (Table 1 and Figure 4).

Table 1. Statistical overview of water-inrush points in mines within the Xinhua mining area.

Coal Mine	Water-Inrush Working Face	Location of Water Inrush	Structure of Water-Inrush Site and Working Face Situation	Water-Inrush Time (Year, Month, Day)	Sudden Water Volume (m^3/h)	Elevation of Water-Inrush Point (Burial Depth) (m)	Water-Inrush Point Number (Marked in Figure 4)
Guiyuan Coal Mine	10,903	276 m has been mined in the middle of the working face	Near the fault	2016.6.16	280	783 (367)	G-1
	10,901	80 m has been mined, and the lower part of the working face	Between two faults	2019.2.30	160	833 (415)	G-2
	10,905	74 m has been mined, and the lower part of the working face	Near the fault	2020.3.10	229	747 (421)	G-3
		143 m has been mined, and the lower part of the working face	Near the fault	2020.5.12	150	751 (436)	G-4
		425 m has been mined, and the lower part of the working face	Near the fault	2020.11.8	290	776 (433)	G-5
	10,908	247 m has been mined, and the lower part of the working face	Normal stratigraphic blocks (slow advancement of the working face)	2021.10.13	210	808 (394)	G-6
		341 m has been mined, and the lower part of the working face	Normal stratigraphic blocks (slow advancement of the working face)	2022.2.14	80	807 (439)	G-7
	2093	161 m has been mined, and the lower part of the working face	Near the fault	2019.7.15	150	728.5 (431.5)	G-8
		237 m has been mined, and the lower part of the working face	Near the fault	2019.11.23	470	729.8 (432.6)	G-9
		270 m has been mined, and the lower part of the working face	Near the fault	2019.12.10	350	730.9 (439.4)	G-10
Jinji Coal Mine	1905	71 m has been mined, and the lower part of the working face	Normal stratigraphic blocks, near the near starting cut of the working face	2018.12.20	200	877.5 (366.1)	J-1
Lindong - Longfeng Coal Mine	5914	202 m has been mined, and the lower part of the working face	Expose the fault location	2019.7.22	160	979.3 (146.2)	L-1
		365 m has been mined, and the lower part of the working face	Normal stratigraphic block, stop mining position	2020.3.24	210	977.8 (127.4)	L-2
Tenglong Coal Mine	1091	163 m has been mined, and the upper part of the working face	40 m normal stratigraphic block segment, 40 m away from the shorting cut of the nearby working face	2020.4.19	80	1047.3 (342.7)	T-1
		536 m has been mined, and the upper part of the working face	Normal geological blocks, slow mining in the working face	2020.11.11	800	1047.4 (350.1)	T-2
	10,903	465 m has been mined, and the lower part of the working face	Near the fault	2022.6.19	Collapse water and gangue	993.4 (274.1)	T-3

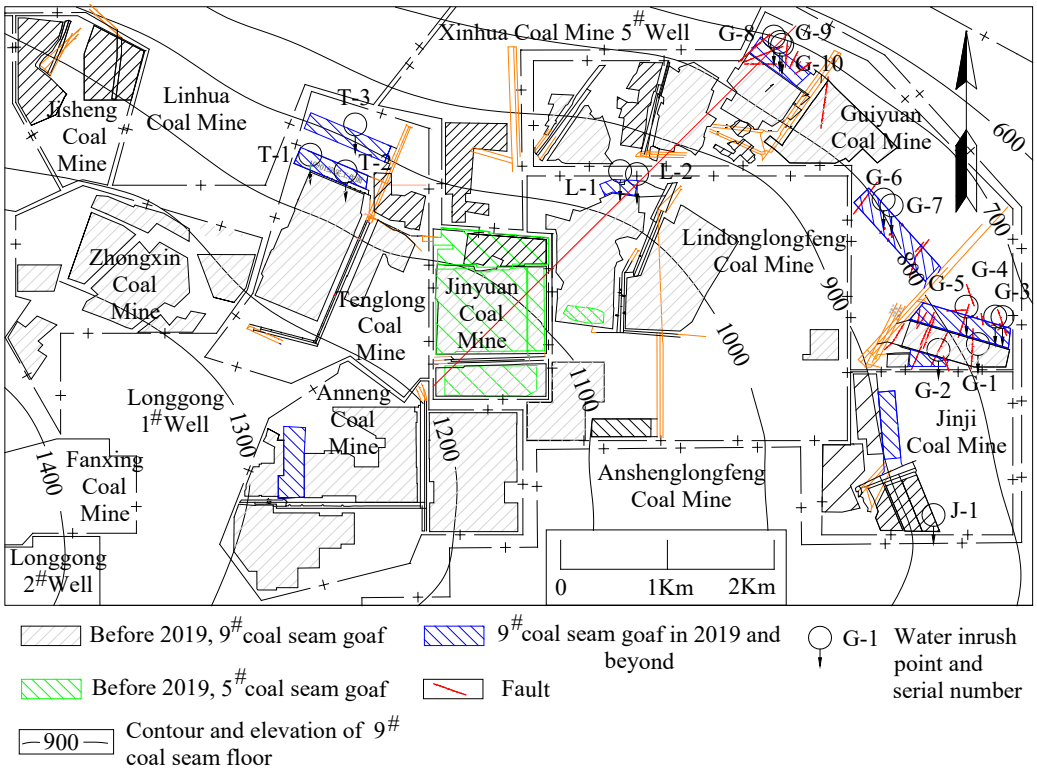

Figure 4. Distribution map of water-inrush points in the working face of Xinhua mining area.

3. Research on Water-Inrush Sources

3.1. Spatial and Temporal Distribution Characteristics of Water Inrush in Working Faces

After nearly 20 years of continuous mining, the coal mines in the area have gradually formed a large goaf extending from the surface coal seam outcrop to the deeper mines. After April 2016, with the large-scale adoption of comprehensive mechanized coal mining technology, the height of coal seam mining has significantly increased compared with traditional blast mining and conventional high-end mining methods. This advancement has facilitated the full-height extraction of moderately thick coal seams in a single operation, with some mines achieving a maximum mining height of 3.6 m. Furthermore, due to the significant increase in the scope of the goaf and the completion of the 9# and 5# coal seams near the shallow outcrop, a large goaf was formed in the mining area. As a consequence of this extensive mining, a large surface mining fracture failure zone emerged [19–22]. Research conducted by Wang Beifang et al. [23] indicated that the fractures generated by mining have also led to primary dissolution gaps and caves within the Changxing Formation rock mass. These fractures, with widths ranging from 0–2.3 m in exposed Changxing Formation limestone on the surface and up to 3 cm in limestone exposed by exploration boreholes, have created pathways for atmospheric precipitation to infiltrate the mining area [2,5,15,24,25]. This infiltration accelerated and increased the volume of water infiltrating the goaf. Consequently, goaf areas with water retention conditions have gradually become direct or indirect water sources capable of inundating the mines. This phenomenon was particularly evident in the central coal mine (mining 9# coal seam) and the Jinyuan Coal Mine (mining 5# and 9# coal seams) located within the large exposed area of the Changxing Formation limestone in the middle of the mining area. In these mines, after the completion of resource extraction, the goaf formed after pit closure served as an extensive reservoir for accumulated water, replenishing the mining area below through the Changxing Formation aquifer (Figure 4).

Each mine in the Xinhua mining area employed a downward mining method to arrange working faces. Initially, shallow working faces were mined. Statistical data indicated that the first water-inrush incident occurred at the 10,903 working face of the Guiyuan Coal Mine on 16 June 2016, with

a water-inrush rate of 280 m^3/h, an elevation of 783 m, and a burial depth of 367 m. Subsequently, after the completion of the last lower limit working face (lower limit elevation 1115.3 m) of the north wing of the 5# coal seam in Jinyuan Coal Mine (wellhead elevation 1201.5 m) in 2019, adjacent mines below the lowest mining elevation of the 5# coal seam experienced roof water-inrush incidents during the mining of the 9# coal seam. These water inrushes ranged from 80 m^3/h to 800 m^3/h, with the elevation of water-inrush point in the 9# coal seam working face of each mine varying from 728.5 m to 1047.4 m, and the burial depth ranged from 127.4 m to 439.4 m (Table 1).

3.2. Chemical Analysis of Water Inflow in the Working Face

In this study, during the exploration period, water samples were collected from the Changxing Formation aquifer, surface water sources, and other locations and then subjected to comprehensive water quality analysis. Furthermore, following water-inrush incidents at the working face, additional samples were collected and sent to qualified third-party water quality testing institutions for comprehensive analysis (Table 2), thus ensuring the accuracy of water quality assessments. Analysis of surface streams and rivers within the mining area indicated that water near the exposed limestone of the Changxing Formation primarily comprised HCO_3·SO_4-Na-type water, with a total dissolved solids content of 515.50 mg/L–907.50 mg/L. Limestone water from the Changxing Formation (sampled at elevation 794.7 m–883.83 m, with burial depth of 333.42 m–409.30 m) was mainly composed of HCO_3·SO_4-Na (Na+K)·Ca, HCO_3·SO_4-Ca·Na (Na+K)-type water, with a total dissolved solids content of 168.00 mg/L–279.50 mg/L. After water inrush on the roof of the working face in the coal mines, a sample (collected at an elevation of 776 m–985 m and buried depth of 172 m–450 m) was subjected to comprehensive analysis, revealing water quality types characterized by HCO_3-Na and HCO_3·SO_4-Na, with a total dissolved solids content of 327.76 mg/L–892.59 mg/L.

Given the data in Table 2, a Piper diagram of the hydrochemical properties of surface water, Changxing Formation limestone water, and water outlet points was drawn according to the Shukarev hydrochemical types [26–28] (Figure 5). According to the Piper plot, surface water was generally located in low-lying areas and eventually flowed into rivers. The water quality was significantly affected by residential activities, correlating with the relevant research by Deshmukh and Keshav K [29]. Upstream areas of the river were mainly supplied by spring water, exhibiting higher Ca^{2+} and Mg^{2+} contents, accounting for over 70% of the cation composition. However, downstream, especially after passing through residential areas, the proportion of sodium ions gradually increased due to increased domestic sewage discharge, and the Na^+ and K^+ content gradually increased from ~27% to over 85%. Analysis of the on-site water intake locations indicated that water sample 3 was collected near the source of the river, which was replenished by limestone spring water in the Yulong Mountain section, exhibiting the highest concentration of Ca^{2+} cations. Water sample 1 was collected from the Changxing Formation outcrop, situated in low-lying terrain and a residential gathering area, with Na^+ dominating the cation composition. Water sample 2 was collected from the limestone formation outcrop in the Yulong Mountain section, indicating a diluted river water composition due to limestone water inrush, resulting in lower Na^+ content and higher Ca^{2+} content.

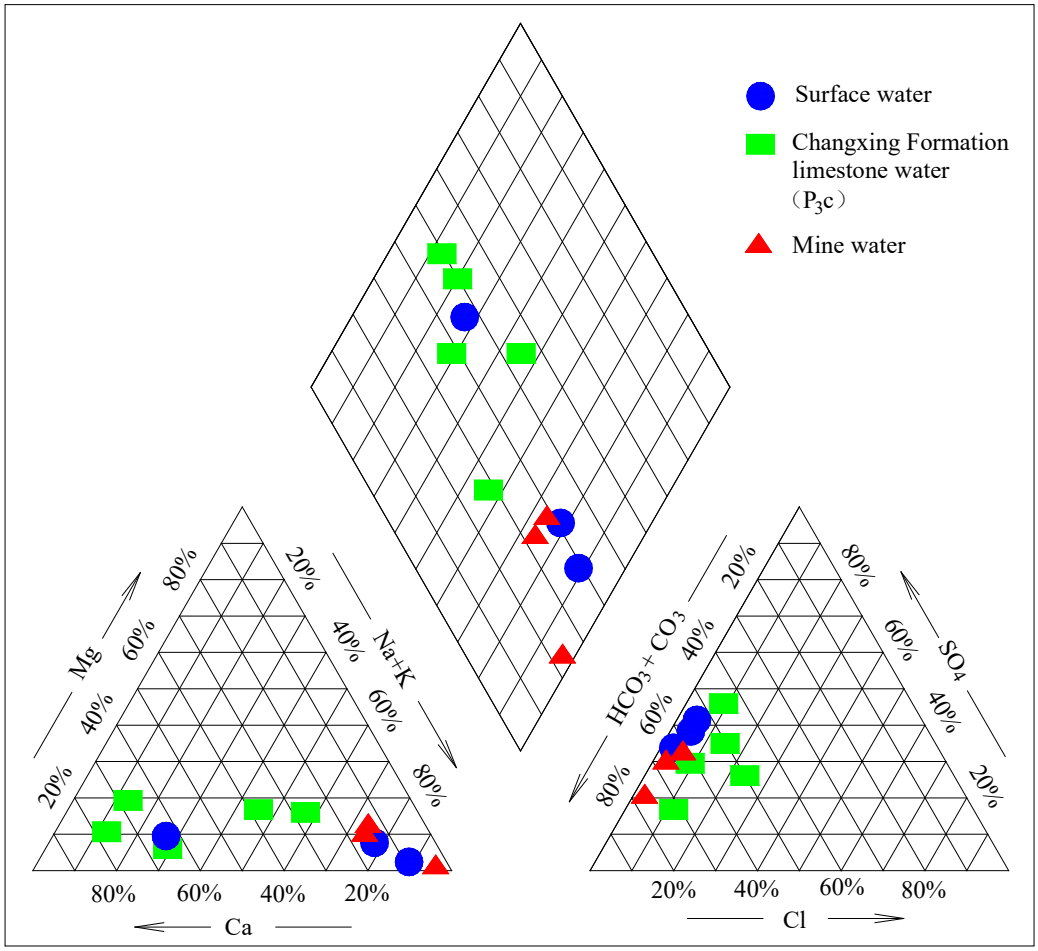

Figure 5. Piper three-line diagram of surface water, karst water, and mine water.

In this study, before being affected by mining damage, the limestone in the Changxing Formation originally experienced slow or even stagnant groundwater flow (hydraulic conductivity 0.0000026 m/d–0.004 m/d) due to undeveloped karst. However, it also experienced relatively fast groundwater flow (hydraulic conductivity of ~0.1079 m/d) in locally developed karst areas. This change altered the water quality type of the limestone in the Changxing Formation from HCO_3·SO_4-Ca water to HCO_3·SO_4-Ca·Na water, which eventually became HCO_3·SO_4-Na·Ca water. The diversity of water quality types in the limestone water of the Changxing Formation indicated that under closed conditions, it primarily comprised HCO_3·SO_4-Ca. Under micro-permeable conditions, it was replenished by surface water, thus changing it to HCO_3·SO_4-Ca·Na water. In areas with karst development, surface water supplied a significant amount of groundwater, and the water quality was significantly affected by human activities. Na^+ was the dominant cation. Furthermore, changes in the water quality of the aquifer in the Changxing Formation indicated that after being damaged by mining activities, the cracks in the limestone became water channels for surface water to supply the mining area.

Table 2. Water quality analysis results of surface water, Changxing Formation limestone water, and mine water.

Water Sample Location		Surface Water (mg/L)			Changxing Formation (P_3c) Limestone Water (mg/L)				Mine Water (mg/L)			
Cation	Ca^{2+}	23.55	45.89	112.04	65.38	17.01	60.17	47.62	52.75	4.80	21.15	15.66
	Mg^{2+}	4.20	14.73	10.20	8.60	6.15	3.40	8.19	14.14	1.46	8.07	8.55

	Na^+	257.83	280.60	54.79	15.54	38.90	30.05	10.60	72.93	344.00	115.00	96.50
	K^+	1.85	2.86		1.33		1.74			7.10	1.30	1.50
	NH_4^+	0.05	0.16	0	0	1.02	0	0	0	2.4	1.0	0.52
	HCO_3^+	469.61	558.68	288.85	142.54	137.53	163.66	106.90	192.09	642.17	249.27	227.40
	CO_3^{2+}	7.24	4.34	0	0	0	0	0	0	45.57	0.00	0.00
Anion	SO_4^{2+}	196.54	305.41	175.34	58.45	25.31	60.81	58.45	153.12	150.00	104.00	80.00
	Cl^+	27.76	9.75	15.07	39.36	12.87	13.51	18.19	22.12	17.29	13.59	6.31
	NO_3^+	3.09	7.56	0.20	0	0.20	5.22	1.77	0.04	0.50	1.98	2.11
	NO_2^+	0.03	0.62	0	0	< 0. 12	0.06	< 0.12	0.24	0.272	<0.10	0.006
Total hardness (mg/L)		77.06	175.24	321.82	200.27	102.72	164.21	152.65	189.98	86.05	86.05	74.31
Total dissolved solids TDS (mg/L)		716.00	907.50	510.50	250.53	144.00	279.50	168.00	430	892.59	393.58	327.76
PH		8.9	8.6	7.17	7.5	7.82	8.4	8.55	6.1	8.18	8.18	8.11
Water quality type		$HCO_3 \cdot SO_4$ -Na	$HCO_3 \cdot SO_4$ -Na	$HCO_3 \cdot SO_4$ -Ca·Na	$HCO_3 \cdot SO_4$ -Ca	HCO_3 -Na·Ca	$HCO_3 \cdot SO_4$ -Ca·Na	$HCO_3 \cdot SO_4$ -Ca·Na	$HCO_3 \cdot SO_4$ -Na·Ca	HCO_3 -Na	$HCO_3 \cdot SO_4$ -Na	$HCO_3 \cdot SO_4$ -Na
Elevation (burial depth) (m)		1171.2	1327.5	1072.8	829.70 (305.86)	1364.46 (21.27)	1038.00 (332.45)	794.70 (322.12)	979.3 (231.5)	945 (450)	776 (419)	985 (172)
Notes		Surface water 1	Surface water 2	Surface water 3	1707 Borehole in Linhua Coal Mine	401 Borehole in Fuliyuan Coal Mine (near the outcrop)	904 Borehole in Linhua Coal Mine	402 Borehole in Guiyuan Coal Mine	B3509-2 Borehole in Anshenglong feng Coal Mine	10,908 Working face of Guiyuan Coal Mine	10,905 Working face of Guiyuan Coal Mine	Water outlet point of Changxing Formation limestone in the main shaft of Guiyuan Coal Mine

The water quality analysis of mine water indicated that the primary water quality type of mine water was $HCO_3 \cdot SO_4$-Na type, which was essentially similar to that of surface water. Therefore, surface water supplied the mine inflow, and the Changxing Formation limestone became a supply channel for surface water and atmospheric precipitation to mine water.

3.3. Analysis of the Correlation between Mine Water Inflow and Atmospheric Precipitation

In this study, due to long-term weathering and erosion by rainwater, low-lying sites and ditches have been gradually formed at the exposed limestone of the Changxing Formation. The river water surface is generally wide, and the water flow is slow, allowing atmospheric precipitation to easily collect and infiltrate. Under long-term dissolution, seasonal streams and gullies were widely distributed near the outcrop of the Changxing Formation (Figure 3). This increased the intensity and duration of atmospheric precipitation as well as surface water infiltration into the Changxing Formation limestone. Studies by Yang Jianhua et al. [30] and Wang Shufang [31] investigated the close relationship between mine water inrush near the shallow outcrop of coal seams and atmospheric precipitation in the karst landform area of Guizhou. Atmospheric precipitation was the main source of mine water supply. Furthermore, during the shallow coal seam mining, atmospheric precipitation rapidly replenished the mine, and the shortest replenishment time was 2 h. As the burial depth of coal seams increased during mining, the distance of atmospheric precipitation from the coal seam outcrop to the underground mining area increased, thus decreasing the replenishment amount and increasing the time. The Changxing Formation limestone was widely exposed near the coal seam outcrop in the Xinhua mining area of Jinsha County (Figure 3). This limestone served as a reservoir for atmospheric precipitation and transported it deep into the mining area through channels such as

dissolution gaps, caves, and fractures in the rock layers. In its original karst fissure state (before it was affected and destroyed by mining), the water supply to the underground mining area of the coal mine through the Changxing Formation limestone was relatively small, and the supply cycle was long. However, after damaging the integrity of the limestone in the shallow mine and completing mining, the water inflow in the deep mine significantly increased. This considerably reduced the time for atmospheric precipitation to supply the underground. For example, after the completion of mining in 2019 at the last 10,508 working face (lower limit elevation 1115.3 m) of the 5# coal seam in the northwest wing of Jinyuan Coal Mine, the mine began to retreat, and the pit was closed. In the deep Guiyuan No.2 mine, the amount of water inflow significantly increased, and the period of atmospheric precipitation recharge was significantly shortened (Figure 6). The water inflow of the mine increased from 84 m^3/h pre-2019 to 242 m^3/h in 2022. Additionally, during the rainy season, the time interval between the peak water inflow in mines and the peak rainfall gradually decreased from ~10 months before 2019 to 6 months in 2020. From 2021 to 2022, the peak water inflow in mines synchronized with the peak rainfall in the same month. This indicated that the secondary cracks generated after coal seam mining activities led to the connection of primary cracks, dissolution cracks, and caves in the Changxing Formation limestone. The unobstructed water storage and supply capacity in the goaf increased the speed and amount of atmospheric precipitation replenishment for mine water.

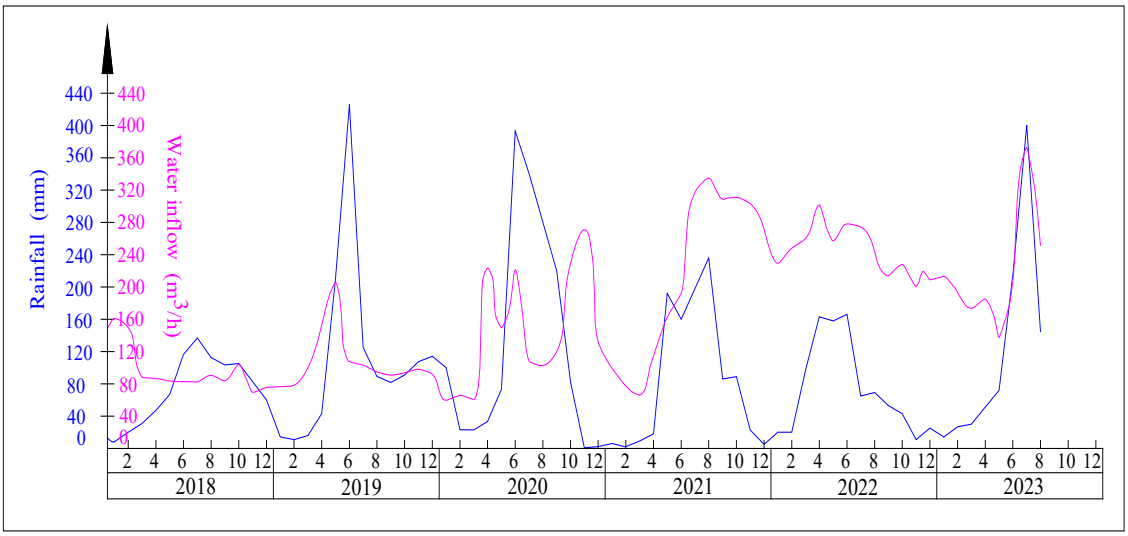

Figure 6. The curve of the relationship between water inflow and atmospheric precipitation at Guiyuan Coal Mine.

4. Mechanism of Underground Stope Replenishment through Atmospheric Precipitation

In its original state, before any mining activity, only certain sections of the Changxing Formation limestone featured dissolution cracks and caves, with minimal crack development. The groundwater permeability coefficient, K, ranged from 0.0000026 m/d to 0.1079 m/d. After atmospheric precipitation infiltration, runoff was sluggish, resulting in a prolonged replenishment cycle for deep aquifers and a limited replenishment volume (Figure 7). Under these groundwater runoff conditions, the Guiyuan coal mine experienced an inflow of ~84 m^3/h, with atmospheric precipitation supplying the mine scope over ~10 months. The predominant cation in the runoff retention area was Ca^{2+}, while Na^+ predominated in the runoff area.

After the completion of mining operations in the 5# and 9# coal seams, extensive goaf formation occurred in the shallow mines within the mining area, leading to well-developed water-conducting fracture zones. These zones provided ample storage capacity and conduits for atmospheric precipitation to supply the mines. The quality of mine inflow water was correlated with that of surface water, with $Na^+(+K^+)$ constituting the primary cation. Atmospheric precipitation smoothly replenished the mining area through the water-conducting fracture zones of the Changxing

Formation limestone until the closure of the shallow mine. Despite significant water inflow into the mine, no water-inrush incidents were reported. Furthermore, during this period, atmospheric precipitation and groundwater primarily sustained the shallow mine, with only a fraction contributing to runoff for the deep mine (Figure 8). Under these groundwater runoff conditions, mine water quality remained consistent with surface water, with $Na^+(+K^+)$ dominating as the main cation.

After the closure of the shallow mine, as water discharge ceased, atmospheric precipitation replenished the Changxing Formation limestone, storing water within the original dissolution gaps, caves, and cracks due to mining activities. Mining-induced cracks facilitated the smooth flow of water within the Changxing Formation limestone, serving as a water source and conduit for water inrushes at the deep mining face. Sediment carried by atmospheric precipitation filled the goaf of the fully mined deep mines, coupled with water immersion and coal-bearing strata mud expansion within the goaf. In the event of a water inrush at the working face, goaf water inflow gradually decreases over time. Typically, post-mining completion, goaf water inflow did not exceed 10 m^3/h. Additionally, accumulated water from the closed shallow mine, goaf, and water-conducting fracture zones in the deep mine flowed into the working face. Thus, during periods in areas with abnormal development of the water-conducting fracture zone before and after the initial pressure on the new working face, in areas where faults develop, in areas where mining is slow, and during periods of mining cessation, these conditions led to another water-inrush incident (Figure 9).

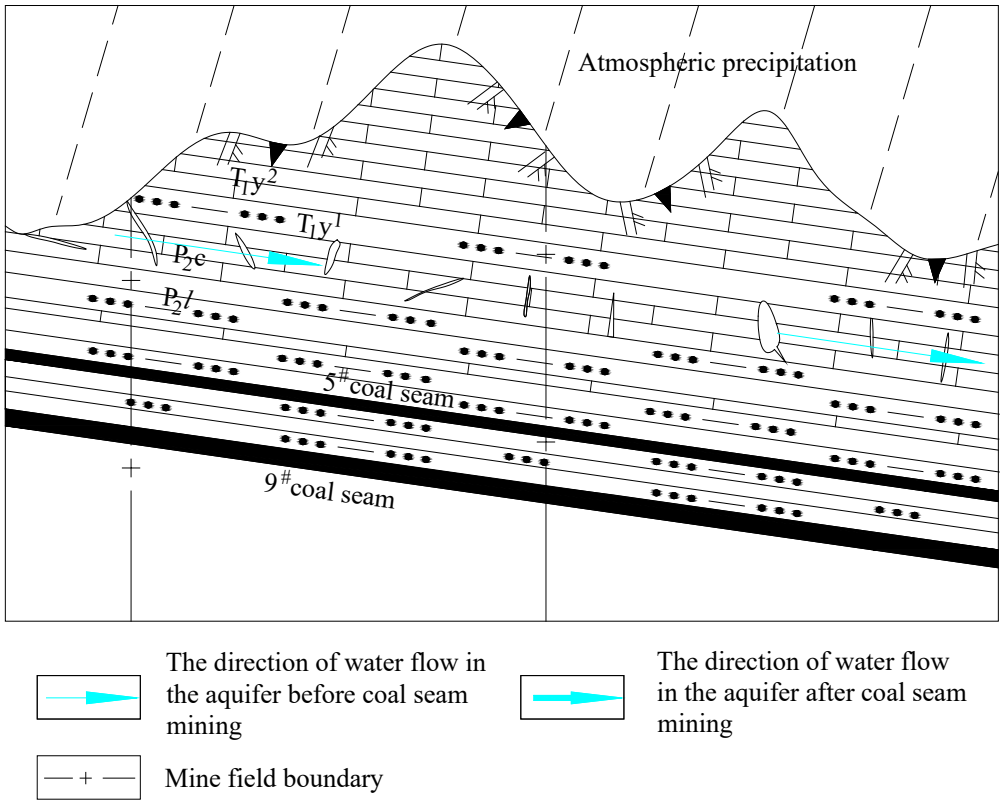

Figure 7. Water runoff map of the limestone in the Changxing Formation in its original state.

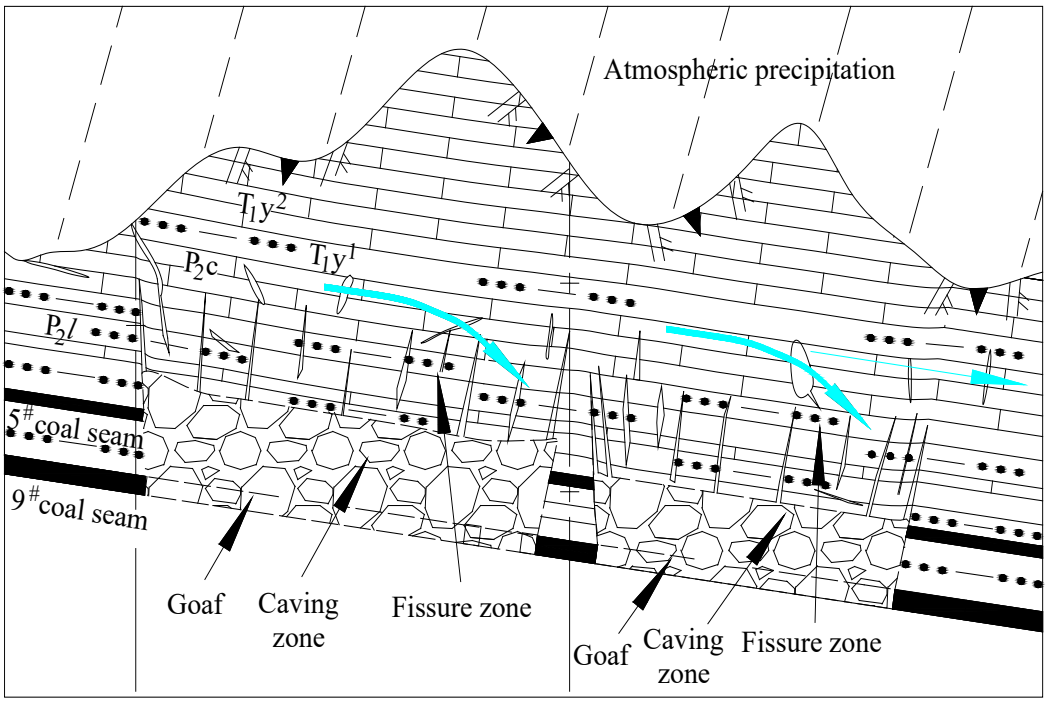

Figure 8. Atmospheric precipitation groundwater recharge before the closure of shallow mines.

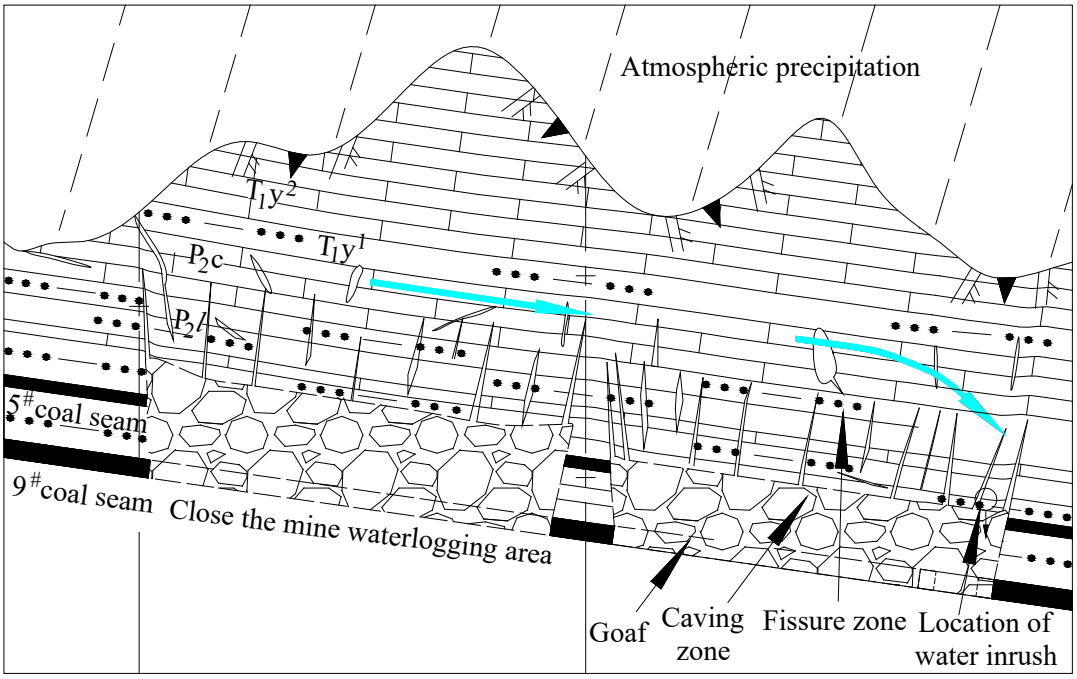

Figure 9. Atmospheric precipitation groundwater recharge map after the closure of shallow mines.

5. Conclusions

(1) The weak water-rich and weakly permeable aquifers in the Changxing Formation limestone were interconnected by cracks and caves formed under mining conditions, enhancing the water richness of the Changxing Formation limestone and transforming it into a huge water storage space. This phenomenon often leads to water-inrush incidents in deep mines.

(2) A hydrochemical connection existed between surface water, the Changxing Formation limestone aquifer water, and mine inflow water. The water quality of mine water and surface water

was consistent, with the original Changxing Formation limestone water exhibiting a transitional between the two.

(3) Mining-induced damage to the Changxing Formation limestone expanded its damage range and water storage capacity, effectively reducing the distance and increasing the intensity with which atmospheric precipitation replenished the mining area. Therefore, atmospheric precipitation emerged as the main source of water influx in existing mines.

(4) The study investigated the mechanism through which atmospheric precipitation replenishes deep mines through the Changxing Formation limestone reservoir and water-conducting channels. However, there remains a lack of in-depth research on the formation mechanism of the Changxing Formation limestone water-conducting channels. Future research on the formation mechanism of these channels will be pivotal in preventing and controlling atmospheric precipitation-induced water damage in deep mines.

Author Contributions: Writing—original draft preparation, X.S.; writing—review and editing, X.S. and S.Z.; formal analysis and funding acquisition, G.X. All authors have read and agreed to publish the manu-script version.

Funding: This research was funded by the Innovation Team of universities in Guizhou Province for mine water disaster prevention and control in southwest karst area. Guizhou education department [2023]092; Engineering research center for coal mine water disaster prevention and control in Bijie region [2023]11.

Data Availability Statement: All data generated or analyzed during this study are included in this article.

Conflicts of Interest: The authors declared that they have no conflicts of interest to this work.

References

1. Song, Z. The Impact and Prediction Analysis of Atmospheric Precipitation on Coal Mine Water Inflow in Southwest Mountain Areas—Taking Xiaotun Mine as an Example. Master's Thesis China University of Mining and Technology, Xuzhou, China, 2019.
2. Suo, J.; Qin, Q.; Wang, W.; Li, Z.; Huang, C.; Xu, Y.; Chen, Z. Disastrous Mechanism of Water Burst by Karst Roof Channel in Rocky Desertification Mining Area in Southwest China. *Geofluids* **2022**, *2022*, 7332182. https://doi.org/10.1155/2022/7332182.
3. Liu, J.; Zhao, Y.; Tan, T.; Zhang, L.; Zhu, S.; Xu, F. Evolution and modeling of mine water inflow and hazard characteristics in southern coalfields of China: A case of Meitanba Mine. *Int. J. Min. Sci. Technol.* **2020**, *32*, 513–524.
4. Wang, H. Prediction of Water Inflow in Huoshaopu Coal Mine in Panxian Basin, Guizhou Province. *China Coal Geol.* **2019**, *31*, 44–51.
5. Shi, X.; Zhang, W. Characteristics of an underground stope channel supplied by atmospheric precipitation and its water disaster prevention in the karst mining areas of Guizhou. *Sci. Rep.* **2023**, *13*, 15892. https://doi.org/10.1038/s41598-023-43209-4.
6. Li, L. Prediction of Mine Pit Water Inflow in Qinglong Coal Mine, Qianxi, Guizhou. *Coal Technol.* **2015**, *34*, 228–230.
7. Mo, L.; Fan, J.; Zhang, G.; Liu, F. Study on inorganic and organic hydrochemical characteristics and water source discrimination in Xiaotun coal mine. *Energy Environ. Prot.* **2019**, *41*, 94–99+104.
8. Zhang, W. Analysis of water drilling technology for exploring top plate sandstone in the 1013 working face of Yushuquan Coal Mine. *Shandong Ind. Technol.* **2015**, *21*, 41.
9. Liang, S. Research on the Distribution Characteristics of Confined Water and Safe Mining Techniques in the Qianbei Mining Area. Ph.D. Thesis, China University of Mining and Technology (Beijing), Beijing, China, 2013.
10. LI, Z., LI, S., DU, F., WANG, W., LI, J., JIAO, Y., & FAN, X. Research on the development law of karst caves on water conducting fractures under the influence of mining in Southwest Karst Mining Areas. *Coal Sci. Technol.* **2023**, *51*, 106–117.
11. Zheng, G. Analysis of the Formation mechanism of water and gangue collapse accidents in Tenglong Coal Mine, Guizhou Province. *China Coal Geol.* **2024**, *36*, 43–46, 5.
12. Jin, M.; Yao, X.; Zhang, W.; Qin, X; Yang, X. Research on the Formation Mechanism and Comprehensive Prevention and Control Technology of Separation Water in Changxing Formation of Qianbei Coalfield. *Coal Technol.* **2023**, *42*, 128–132.

13. Li, B.; Wei, T.; Liu, Z. Construction of evaluation index system for water abundance of karst aquifers and risk assessment of water inrush on coal seam roof in Southwest China. *J. China Coal Soc.* **2022**, *47*, 152–159.
14. Shi, X.; Qian, Z.; Li, T.; Jiang, Z.; Jiang, T. Study on the occurrence characteristics of karst groundwater in coal measures Roof. *Coal Eng.* **2017**, *49*, 63–66.
15. Yao, G.; Chen, Z.; Xiang, X. Research on the characteristics of water barrier damage and surface water infiltration under coal mining conditions in karst mountainous areas. *Hydrogeol. Eng. Geol.* **2012**, *39*, 16–20+25.
16. Wang, Z.; Zhang, Q.; Zhang, W. A novel collaborative study of abnormal roof water inrush in coal seam mining base d on strata separation and wing crack initiation. *Eng. Fail. Anal.* **2022**, *142*, 106762. https://doi.org/10.1016/j.engfailanal.2022.106762.
17. Long, T.; Hou, E.; Xie, X.; Fan, Z.; Tan, E. Study on the damage characteristics of overburden of mining roof in deeply buried coal seam. *Sci. Rep.* **2022**, *12*, 11141. https://doi.org/10.1038/s41598-022-15220-8.
18. Xiao, L.; Li, F.; Niu, C.; Dai, G.; Qiao, Q.; Lin, C. Evaluation of Water Inrush Hazard in Coal Seam Roof Based on the AHP-CRITIC Composite Weighted Method. *Energies* **2023**, *16*, 114. https://doi.org/10.3390/en16010114.
19. Liu, H.; Deng, K.; Zhu, X.; Jiang, C. Effects of mining speed on the developmental features of mining-induced ground fissures. *Bull. Eng. Geol. Environ.* **2019**, *78*, 6297–6309. https://doi.org/10.1007/s10064-019-01532-z.
20. Li, X.; Ji, D.; Han, P.; Li, Q.; Zhao, H.; He, F. Study of water-conducting fractured zone development law and assessment method in longwall mining of shallow coal seam. *Sci. Rep.* **2022**, *12*, 7994. https://doi.org/10.1038/s41598-022-12023-9.
21. Zhai, W.; Li, W.; Huang, Y.; Ouyang, S.; Ma, K.; Li, J.; Gao, H.; Zhang, P. A Case Study of the Water Abundance Evaluation of Roof Aquifer Based on the Development Height of Water-Conducting Fracture Zone. *Energies* **2020**, *13*, 4095. https://doi.org/10.3390/en13164095.
22. Wang, W.; Li, Z.; Du, F.; Cao, Z.; Li, G. Study of Roof Water Inrush Control Technology and Water Resources Utilization During Coal Mining in a Karst Area. *Mine Water Environ.* **2023**, *42*, 546–559. https://doi.org/10.1007/s10230-023-00953-3.
23. Wang, B.; Zhou, D.; Zhang, J.; Liang, B. Research on the dynamic evolution law of fssures in shallow-buried and short-distance coal seam mining in Lijiahao Coal Mine. *Sci. Rep.* **2023**, *13*, 5625. https://doi.org/10.1038/s41598-023-32849-1.
24. Zhu, C.; Cui, D.; Zhou, Z.; Li, Q.; Huang, Y. Similar simulation of mining-induced fissure development law and cave destruction character when mining in karst area. *J. Undergr. Space Eng.* **2019**, *15*, 93–100+124.
25. Liu, Q.; Zhou, C.; Ma, D.; Liu, Y.; Wang, G.; Huang, Z. Evolution of Water-Conducting Fracture in Weakly Cemented Strata in Response to Mining Activity: Insights from Experimental Investigation and Numerical Simulation. *Water* **2023**, *15*, 4173. https://doi.org/10.3390/w15234173.
26. Chen, W.; Zeng, C.; Gong, X.; Tai, Z.; Deng, J.; Yang, M. Hydrological and hydrochemical regime of a typical subterraneous river in a deep canyon karst area: A case study in the Santang underground river, Guizhou. *Hydrogeol. Eng. Geol.* **2022**, *49*, 19–29. https://doi.org/10.16030/j.cnki.issn.1000-3665.202109047.
27. Han, J.; Gao, J.; Du, K.; Chen, M.; Jiang, B.; Zhang, K. Analysis of hydrochemical characteristics and formation mechanismin coal mine underground reservoir. *Coal Sci. Technol.* **2020**, *48*, 223–231.
28. Bian, Z.; Cui, Y.-J.; Li, J.; Du, J.-G. Quality Assessment and Hydrogeochemistry of Surface Water in the Liujiang Basin, Hebei Province. *Bull. Mineral. Petrol. Geochem.* **2019**, *38*, 953–960. https://doi.org/10.19658/j.issn.1007-2802.2019.38.122.
29. Deshmukh, K.K. Impact of Human Activities on the Quality of Groundwater from Sangamner Area, Ahmednagar District, Maharashtra, India. *Int. Res. J. Environ. Sci.* **2013**, *2*, 66–74.
30. Yang, J.; Cai, Y. Analysis of dynamic influencing factors of mine water inflow—Taking a coal mine in Guizhou as an example. *Water Conserv. Sci. Technol. Econ.* **2021**, *27*, 61–65+76.
31. Wang, S. Research progress of precipitation infiltration supplement in karst aquifer system. *J. China Hydrol.* **2014**, *34*, 1–8.